

A thermo-micro-mechanical modeling for smart shape memory alloy woven composite under in-plane biaxial deformation

Hossein Ali Sepiani · Asdollah Ghazavi

Received: 14 May 2008 / Accepted: 11 September 2008 / Published online: 11 October 2008
© Springer Science+Business Media, B.V. 2008

Abstract This paper presents a theoretical study of the in-plane behavior of Smart Shape Memory Alloy Woven Composites (SSMAWC) under biaxial loading by developing an integrated micromechanical constitutive model. The model studied in this research is established on the geometric parameters of fibers, metal layers, unit cell, the material constants of composite constituents, and the orientation of fibers, in which the fibers in one direction are SMA ones. The Helmholtz free energy of a Shape Memory Alloy, in 3-Dimensional and 1-Dimensional applications is derived. Using mechanical energy of matrix and elastic yarns, the constitutive relations are developed with the use of strain energy approach and energy variation theorem. The kinetic relations of SMA depicted by Brinson is coupled with the final governing equation of the composite to predict the stress history in smart shape memory alloy woven composites. The deflection of the structure, subjected to uniform biaxial loading is studied numerically. It is found that the effect of Shape Memory Effect (SME) of the SMA wires on the behavior of plain woven flexible fabric composite is significant.

Keywords Smart shape memory alloy woven composite · Helmholtz free energy · Strain energy

1 Introduction

In recent years, many researchers have devoted their attentions on a special class of material, the shape memory alloy (SMA). As is well known, if the alloy is trained to have a particular shape in austenite phase, it is capable of memorizing this shape. A large plastic deformation can be produced when the alloy is subjected to external force due to martensite transformation. If it is then heated above the austenite transformation temperature and restrained to contract, a large recovery force arises out of the phase transformation from martensite to austenite. Because of this unique property, SMA is prospective in many exciting and innovative engineering applications such as structural vibration control, buckling control, and shape control.

Many researchers have conducted investigations of the basic performances and applications of shape memory alloys (SMAs). Therefore, there have been many results of research on SMAs (Gao et al. 2000a, b; Gao and Catherine 2002; Brinson et al. 1999; Brinson and Lammering 1993; Brocca et al. 1999). A general 3-D multivariant micromechanical model for shape memory alloy constitutive behavior was

H. A. Sepiani (✉) · A. Ghazavi
Mechanical Engineering Faculty, University of Tehran,
Tehran, Iran
e-mail: sepiani@ut.ac.ir

A. Ghazavi
e-mail: aghazavi@yahoo.com

developed by Gao et al. (2000a, b) and Gao and Catherine (2002). Brinson et al. (1999) studied the evolution of temperature and deformation profiles seen in SMA wires under specific thermal and mechanical boundary conditions using a macro-scale, phenomenological constitutive model for shape memory alloys in conjunction with energy balance equations. She, also, developed a nonlinear finite element procedure which incorporates a thermodynamically derived constitutive law for SMA material behavior (Brinson and Lammering 1993). Brocca et al. (1999) proposed a model for the behavior of polycrystalline memory alloys (SMA), based on a statically constrained microplane theory.

Additionally, advances in design and manufacturing technologies have greatly enhanced the use of advanced composite materials for aircraft and aerospace structural applications. Due to their structural advantages of high stiffness-to-weight strength-to-weight ratios, composite materials can be used in the design of smart structures and hence significantly improve the performance of aircraft and space structures. In recent years, some researchers have studied shape memory alloy composites (SMACs), which consist of SMA reinforcement and a metal or polymer matrix (Lagoudas et al. 1994; Kawai et al. 1999; Murasawa et al. 2004; Khalili et al. 2007a, b; Yongsheng and Shuangshuang 2007; Zhou et al. 2004; Dano and Hyer 2003). In particular, considerable attention has been paid to development of several analytical and numerical models for the laminated composite structures with integrated SMA sensors and actuators. Lagoudas et al. (1994) and Kawai et al. (1999) proposed the constitutive equation of SMAC to predict its mechanical behavior. The present authors (Murasawa et al. 2004) reported the fracture behavior under uniaxial tension and the deformation behavior under thermo-mechanical loading on NiTi fiberreinforced polycarbonate composites. Khalili et al. (2007a, b) investigated the effect of some important parameters on low-velocity impact response of the active thin-walled hybrid composite plates embedded with the SMA wires employing the first-order shear deformation theory as well as the Fourier series method. Yongsheng and Shuangshuang (2007) studied the free and forced vibration of large deformation composite plate embedded with SMA fibers with use of thermo-mechanical constitutive equation of SMA proposed by Brinson et al. (1999). Zhou et al. (2004)

investigated through-the-thickness mechanical properties of smart quasi-isotropic carbon/epoxy laminates and Dano and Hyer (2003) developed a theory and designed experiments to study the concept of using shape memory alloy (SMA) wires to effect the snap-through of unsymmetric composite laminates.

In addition, over the last four decades or so, a great number of micromechanics models have been proposed in the literature in order to investigate the behavior of woven composites. Surveys about these models can be found, among others, in Refs. (Chamis and Sendeckyj 1968; Hashin 1979; Hashin 1983; Halpin 1992; McCullough 1990). Most these models can be used to accurately estimate the linear elastic property of a fibrous composite. The complex relationship between the fiber properties and the composite behavior has been explored through many theoretical studies as well as experimental ones. Among approaches investigated are the 3D finite element method in conjunction with a micromechanical model (Boisse et al. 1997; Kollegal and Sridharan 2000) and the homogenization method (Hsiao and Kikuchi 1999; Peng and Cao 2002). Luo and Mitra (1995a, b) and Luo and Chou (1986), presented a comprehensive model for woven fabric flexible composites based on the fiber diameter, fiber length in the unit cell, fiber physical property and matrix viscosity. In this model, constitutive relations are derived by means of strain–energy approach and energy variation theorem. Luo’s model can serve as an important guide to further modeling.

Although the laminated composite structures with integrated SMA fibers has been taken up by many aforementioned researchers (Lagoudas et al. 1994; Kawai et al. 1999; Murasawa et al. 2004; Khalili et al. 2007a; Khalili et al. 2007b; Yongsheng and Shuangshuang 2007; Zhou et al. 2004; Dano and Hyer 2003), no work is available on the modeling of smart shape memory alloy woven composites and even that is limited to the modeling of woven fabric composites under large deformation; namely; Luo and Mitra (1995a) and Xue et al. (2005). One means of generating relevant design data is to investigate prototype structures. It is well recognized, however, that prototype testing can be expensive, particularly if it involves the destruction of the test component. Recently, there has been a growing interest in the use of modeling methods to understand and foreseen the behavior of engineering structures.

This paper aims to develop an integrated micro-mechanical constitutive model to predict the in-plane behavior of SSMAWCs under biaxial loading based on the geometric parameters of fibers, metal layers, unit cell, the material constants of composite constituents, and the orientation of fibers. The modeling strategy starts with developing 1D Helmholtz free energy relation for SMA fibers. In this way, based on the first and second law of thermodynamics and Maxwell relations, variations of main parameters about some equilibrium (initial) values will be examined by using a Taylor series approximation. Then, the strategy follows with a geometric description of the yarn and fibers are assumed to be in sinusoidal shape. Following the prospects of Luo and Mitra (1995a, b) and Luo and Chou (1986), the strain energy of consistent are calculated and based on strain energy approach and energy variation theorem, the constitutive equations are derived for SSMAWCs. By such an analysis it is intended to form an opinion about thermo-elastic behavior of laminated plates used in engineering problems associated with such structural designs. Finally, with use of constitutive kinetic relations of SMA fibers, developed by Brinson (1999) and Brinson and Lammering (1993), a numerical study is carried out in order to solve the final constitutive equations in some arbitrary cases. The comparison between numerical and FEM results show good agreement.

2 Definition of the problem

The selection of the unit cell is essential for an appropriate description of composite structures by a micromechanical model. To describe a woven metal laminate composite a 3D unit cell seems to be most suitable because the waviness of the fibers in both directions can be taken into account using this cell. If a reliable constitutive equation for a unit cell is established, the force-deformation of the whole composite's structures can be determined. Considering the fiber arrangement to be periodical, the unit cell of Fig. 1 can be used to characterize a 3D woven composite. The unit cell comprises wavy SMA and elastic fibers which lie in x and y directions respectively and soft matrix surrounding the fibers.

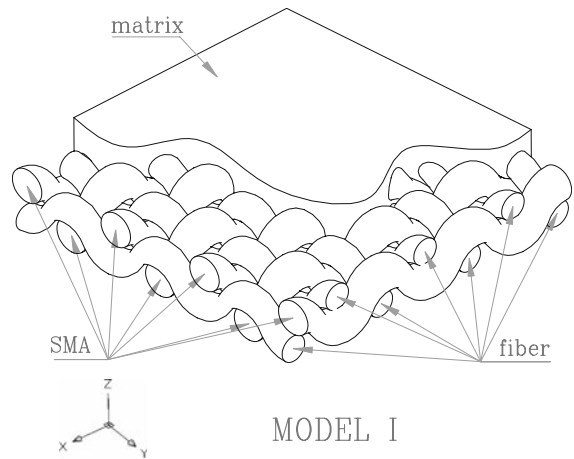


Fig. 1 3D illustration of arrangement of SMA and nylon fibers in the matrix

2.1 Biaxial deformation of a unit cell

The position of the central line of a yarn is mathematically presented as

$$z = a_{\xi} \sin\left(\frac{2\pi\xi}{L_{\xi}}\right) \tag{1}$$

here ξ refers to x or y direction. a_{ξ} and L_{ξ} represent the amplitude and wavelength of the curved yarn in ξ direction. The total length of the unit wavelength in ξ direction can be expressed as

$$S_{\xi} = \int_0^L \sqrt{1 + \left(\frac{2\pi\xi}{L_{\xi}}\right)^2 \cos^2\left[\left(\frac{2\pi\xi}{L_{\xi}}\right)\right]} d\xi \tag{2}$$

For mathematical simplicity (Luo and Chou 1986)

$$\frac{S}{L} = 1 + 9.6\left(\frac{a}{L}\right)^2 - 49.2\left[\left(\frac{a}{L}\right)^2\right]^2 \tag{3}$$

The overall in-plane deformation of the unit cell in Lagrangian strains (Ugural 1990) are:

$$\begin{aligned} E_{11} &= \frac{1}{2}(g_{11}^2 + g_{21}^2 - 1) \\ E_{22} &= \frac{1}{2}(g_{12}^2 + g_{22}^2 - 1) \\ E_{12} = E_{21} &= \frac{1}{2}(g_{11}g_{12} + g_{21}g_{22}) \end{aligned} \tag{4}$$

and the g_{ij} are deformation gradients that are expressed as:

$$g_{11} = L_x/L_{x0}, \quad g_{22} = L_y/L_{y0}, \quad g_{12} = g_{21} = 0 \quad (5)$$

where L_ξ and $L_{\xi 0}$ are the dimensions of the unit cell before and after deformation.

With above equations, the current total length S_ξ of a deformed yarn can be defined by its current amplitude (a_ξ) and wavelength (L_ξ). Thus, the average axial engineering strain of the yarn is expressed as:

$$\begin{aligned} \varepsilon_{f\zeta} &= \frac{S_\xi - S_{\xi 0}}{S_{\xi 0}} \\ &= \frac{L_\xi}{S_{\xi 0}} \left[1 + 9.6 \left(\frac{a_\xi}{L_\xi} \right)^2 - 49.2 \left(\frac{a_\xi}{L_\xi} \right)^4 \right] - 1 \end{aligned} \quad (6)$$

in which

$$\begin{aligned} a_x &= a_{x0}(1 + \varepsilon_z) - \delta \\ a_y &= a_{y0}(1 + \varepsilon_z) + \delta \end{aligned} \quad (7)$$

and δ is the displacement of contact point of warp and yarn.

The mid-plane lateral deflection (w) of the unit cell may be described by a double sine function:

$$w = \delta \sin\left(\frac{2\pi x}{L_{x0}}\right) \sin\left(\frac{2\pi y}{L_{y0}}\right) \quad (8)$$

3 Theoretical analysis

In fact, the condition of a material can be described totally in terms of intensive and extensive parameters. The condition of SMA material can be described in terms of three extensive parameters that are entropy, strain and Martensite fraction. There are extensive parameters (in front of each extensive) that can be used instead of extensive parameters (i.e., temperature, stress field, and phase transformation field).

The Brinson model is based on Tanaka and Nagaki's model. Tanaka and Nagaki developed a model with using of thermodynamical concept of Helmholtz Free Energy. Therefore, we use the Helmholtz Free Energy in which the independent variables are T (temperature), σ_{ij} (stress) and ζ (martensite fraction). Here, the procedures are following: The first law of thermodynamics is given by the following:

$$dU = dQ + dW, \quad (9)$$

where dQ is the heat given to the unit volume of the crystal and dW is the work done on a unit volume of

the crystal. The internal energy (U) is defined by the total amount of energy unaccounted for by gravitational potential energy and kinetic energy. The second law of thermodynamics states that the following is true:

$$dS \geq \frac{dQ}{T} \quad (10)$$

where T is the absolute temperature and S is the systems' final entropy. The greater sign is used for an irreversible process while the equal to sign is used for a reversible process. The work term is the amount of work done on a crystal by both deformation and phase transformation. The work can be written as:

$$dW = \sigma_{ij} d\varepsilon_{ij} + \psi d\zeta \quad (11)$$

where $\sigma_{ij} d\varepsilon_{ij}$ is the work done by deformation and $\psi d\zeta$ is the work done by phase transformation. σ_{ij} , ε_{ij} , ψ , and ζ are the stress field, strain, transformation field and Martensite fraction respectively. Substituting Eqs. 10 and 11 into 9 and considering a reversible process gives the first law of thermodynamics for a SMA material.

$$dU = TdS + \sigma_{ij}d\varepsilon_{ij} + \psi d\zeta \quad (12)$$

Since the internal energy is an exact (or perfect) differential it can be written as the following:

$$dU = \left(\frac{\partial U}{\partial S}\right) dS + \left(\frac{\partial U}{\partial \varepsilon_{ij}}\right) d\varepsilon_{ij} + \left(\frac{\partial U}{\partial \zeta}\right) d\zeta \quad (13)$$

Comparing Eqs. 12 and 13 yields;

$$\begin{aligned} T &= \left(\frac{\partial U}{\partial S}\right)_{\varepsilon_{ij}, \zeta} \\ \sigma_{ij} &= \left(\frac{\partial U}{\partial \varepsilon_{ij}}\right)_{S, \zeta} \\ \psi &= \left(\frac{\partial U}{\partial \zeta}\right)_{\varepsilon_{ij}, S} \end{aligned} \quad (14)$$

The subscripts indicate the variables to be held constant during the differentiation. Thus when a system is described by independent variables (S , ε_{ij} , and ζ) the other variables can be given by first derivatives of the internal energy (U). In general all of the energy functions are properties because they are sums of properties. Since a property can be represented by an exact differential, it can be written in terms of partial derivatives of the appropriate variables. Considering the Helmholtz free energy (A) we have the following:

$$dA = \left(\frac{\partial A}{\partial T}\right) dT + \left(\frac{\partial A}{\partial \varepsilon_{ij}}\right) d\varepsilon_{ij} + \left(\frac{\partial A}{\partial \zeta}\right) d\zeta \tag{15}$$

Since $dU = dA + d(TS)$, therefore, the differential of the Helmholtz free energy, can also be expressed as

$$dA = dU - TdS - SdT \tag{16}$$

Substituting the first law of thermodynamics Eq. 12 into Eq. 16 yields

$$dA = -SdT + \sigma_{ij}d\varepsilon_{ij} + \psi d\zeta \tag{17}$$

If we hold the strain and the martensite fraction constant then those terms in Eq. 15 vanish. We can then equate the remnants of Eq. 15 to 17. This yields the following relationship.

$$-S = \left(\frac{\partial A}{\partial T}\right)_{\varepsilon_{ij}, \zeta} \tag{18}$$

Similarly, the other expressions can be calculated

$$\begin{aligned} \sigma_{ij} &= \left(\frac{\partial A}{\partial \varepsilon_{ij}}\right)_{T, \zeta} \\ \psi &= \left(\frac{\partial A}{\partial \zeta}\right)_{\varepsilon_{ij}, T} \end{aligned} \tag{19}$$

In addition, the Maxwell relations can be calculated as well.

3.1 Linear parameter relationships

Now that we have shown how to relate the variables to the appropriate energy function, we can now derive the shape memory alloy constitutive relationships directly. We can use a Taylor Series approximation to examine variations of these values about some equilibrium (or initial) value. In the way we will use three variables to describe A.

where T_0 , ζ_0 and ε_{ij0} are the equilibrium values of change in temperature, martensite fraction and strain respectively and are represented by Q_0 . It should be noted that all of the derivative terms are evaluated at the equilibrium state Q_0 and thus they are constant terms. Therefore, the coefficients of the change in temperature, strain and martensite fraction are given by equation

$$\begin{aligned} -S|_{Q_0} &= \left(\frac{\partial A}{\partial T}\right)_{Q_0} = -S_0, \quad \sigma_{ij}|_{Q_0} = \left(\frac{\partial A}{\partial \varepsilon_{ij}}\right)_{Q_0} \\ &= \sigma_{ij0}, \quad \psi|_{Q_0} = \left(\frac{\partial A}{\partial \zeta}\right)_{Q_0} = \psi_0 \end{aligned} \tag{21}$$

This means that the linear terms in Eq. 20 will go to zero or a constant. We can now apply Eqs. 18, 19, and 21 to Eq. 20 to obtain

$$\begin{aligned} \frac{\partial A}{\partial T} &= -S \\ &= -S_0 + \left(\frac{\partial^2 A}{\partial T^2}\right)_{Q_0} (T - T_0) \\ &\quad + \left(\frac{\partial^2 A}{\partial T \partial \varepsilon_{ij}}\right)_{Q_0} (\varepsilon_{ij} - \varepsilon_{ij0}) \\ &\quad + \left(\frac{\partial^2 A}{\partial T \partial \zeta}\right)_{Q_0} (\zeta - \zeta_0) \end{aligned} \tag{22}$$

Simplifying yields

$$\begin{aligned} -ds &= -S + S_0 \\ &= \left(\frac{\partial^2 A}{\partial T^2}\right)_{Q_0} (T - T_0) + \left(\frac{\partial^2 A}{\partial T \partial \varepsilon_{ij}}\right)_{Q_0} (\varepsilon_{ij} - \varepsilon_{ij0}) \\ &\quad + \left(\frac{\partial^2 A}{\partial T \partial \zeta}\right)_{Q_0} (\zeta - \zeta_0) \end{aligned} \tag{23}$$

Applying the second and third terms in Eq. 21 gives

$$\begin{aligned} A &= A_0 + \left(\frac{\partial A}{\partial T}\right)_{Q_0} (T - T_0) + \left(\frac{\partial A}{\partial \varepsilon_{ij}}\right)_{Q_0} (\varepsilon_{ij} - \varepsilon_{ij0}) + \left(\frac{\partial A}{\partial \zeta}\right)_{Q_0} (\zeta - \zeta_0) \\ &\quad + \frac{1}{2} \left[\left(\frac{\partial^2 A}{\partial T^2}\right)_{Q_0} (T - T_0)^2 + \left(\frac{\partial^2 A}{\partial \varepsilon_{ij} \partial \varepsilon_{kl}}\right)_{Q_0} (\varepsilon_{ij} - \varepsilon_{ij0}) (\varepsilon_{kl} - \varepsilon_{kl0}) + \left(\frac{\partial^2 A}{\partial \zeta^2}\right)_{Q_0} (\zeta - \zeta_0)^2 \right] \\ &\quad + \left[\left(\frac{\partial^2 A}{\partial T \partial \varepsilon_{ij}}\right)_{Q_0} (T - T_0) (\varepsilon_{ij} - \varepsilon_{ij0}) + \left(\frac{\partial^2 A}{\partial \varepsilon_{ij} \partial \zeta}\right)_{Q_0} (\varepsilon_{ij} - \varepsilon_{ij0}) (\zeta - \zeta_0) + \left(\frac{\partial^2 A}{\partial T \partial \zeta}\right)_{Q_0} (T - T_0) (\zeta - \zeta_0) \right] \end{aligned} \tag{20}$$

$$\begin{aligned} \sigma_{ij} &= \left(\frac{\partial A}{\partial \varepsilon_{ij}}\right) = \sigma_{ij0} + \left(\frac{\partial^2 A}{\partial T \partial \varepsilon_{ij}}\right)\bigg|_{Q_0} (T - T_0) \\ &+ \left(\frac{\partial^2 A}{\partial \varepsilon_{ij} \partial \varepsilon_{kl}}\right)\bigg|_{Q_0} (\varepsilon_{kl} - \varepsilon_{kl0}) + \left(\frac{\partial^2 A}{\partial \varepsilon_{ij} \partial \zeta}\right)\bigg|_{Q_0} (\zeta - \zeta_0) \end{aligned} \tag{24}$$

$$\begin{aligned} \psi &= \left(\frac{\partial A}{\partial \zeta}\right) = \psi_0 + \left(\frac{\partial^2 A}{\partial T \partial \zeta}\right)\bigg|_{Q_0} (T - T_0) \\ &+ \left(\frac{\partial^2 A}{\partial \varepsilon_{ij} \partial \zeta}\right)\bigg|_{Q_0} (\varepsilon_{ij} - \varepsilon_{ij0}) + \left(\frac{\partial^2 A}{\partial \zeta^2}\right)\bigg|_{Q_0} (\zeta - \zeta_0) \end{aligned} \tag{25}$$

3.2 The energy relations for a SMA wire in 1D

To model SMA fibers in the composite, we use 1D model of Brinson, in which stress and strain are functions of “x”. Therefore, Eq. 20 can be reduced to:

$$\begin{aligned} A_{1-D} &= A_0 + \left(\frac{\partial A_{1-D}}{\partial T}\right)_{Q_0} (T - T_0) + \left(\frac{\partial A_{1-D}}{\partial \varepsilon_x}\right)_{Q_0} (\varepsilon_x - \varepsilon_{x0}) + \left(\frac{\partial A_{1-D}}{\partial \zeta}\right)_{Q_0} (\zeta - \zeta_0) \\ &+ \frac{1}{2} \left[\left(\frac{\partial^2 A_{1-D}}{\partial T^2}\right)_{Q_0} (T - T_0)^2 + \left(\frac{\partial^2 A_{1-D}}{\partial \varepsilon_x^2}\right)_{Q_0} (\varepsilon_x - \varepsilon_{x0})^2 + \left(\frac{\partial^2 A_{1-D}}{\partial \zeta^2}\right)_{Q_0} (\zeta - \zeta_0)^2 \right] \\ &+ \left[\left(\frac{\partial^2 A_{1-D}}{\partial T \partial \varepsilon_x}\right)_{Q_0} (T - T_0)(\varepsilon_x - \varepsilon_{x0}) + \left(\frac{\partial^2 A_{1-D}}{\partial \varepsilon_x \partial \zeta}\right)_{Q_0} (\varepsilon_x - \varepsilon_{x0})(\zeta - \zeta_0) \right. \\ &\left. + \left(\frac{\partial^2 A_{1-D}}{\partial T \partial \zeta}\right)_{Q_0} (T - T_0)(\zeta - \zeta_0) \right] \end{aligned} \tag{26}$$

Also for Eqs. 23, 24, and 25 we have:

$$\begin{aligned} -S &= \left(\frac{\partial A_{1-D}}{\partial T}\right) = -S_0 + \left(\frac{\partial^2 A_{1-D}}{\partial T^2}\right)\bigg|_{Q_0} (T - T_0) \\ &+ \left(\frac{\partial^2 A_{1-D}}{\partial T \partial \varepsilon_x}\right)\bigg|_{Q_0} (\varepsilon_x - \varepsilon_{x0}) + \left(\frac{\partial^2 A_{1-D}}{\partial T \partial \zeta}\right)\bigg|_{Q_0} (\zeta - \zeta_0) \end{aligned} \tag{27}$$

$$\begin{aligned} \sigma_x &= \left(\frac{\partial A_{1-D}}{\partial \varepsilon_x}\right) = \left(\frac{\partial^2 A_{1-D}}{\partial \varepsilon_x^2}\right)\bigg|_{Q_0} (\varepsilon_x - \varepsilon_{x0}) \\ &+ \left(\frac{\partial^2 A_{1-D}}{\partial \varepsilon_x \partial \zeta}\right)\bigg|_{Q_0} (\zeta - \zeta_0) + \left(\frac{\partial^2 A_{1-D}}{\partial T \partial \varepsilon_x}\right)\bigg|_{Q_0} (T - T_0) \end{aligned} \tag{28}$$

$$\begin{aligned} \psi &= \left(\frac{\partial A_{1-D}}{\partial \zeta}\right) = \left(\frac{\partial^2 A_{1-D}}{\partial T \partial \zeta}\right)\bigg|_{Q_0} (T - T_0) \\ &+ \left(\frac{\partial^2 A_{1-D}}{\partial \varepsilon_x \partial \zeta}\right)\bigg|_{Q_0} (\varepsilon_x - \varepsilon_{x0}) + \left(\frac{\partial^2 A_{1-D}}{\partial \zeta^2}\right)\bigg|_{Q_0} (\zeta - \zeta_0) \end{aligned} \tag{29}$$

where it is assumed that the stress and transformation field are zero at the equilibrium state and they are chosen as a starting point.

4 Calculation of total energy of a smart unit cell

Due to the nonhomogenous deformation within the unit cell, the strain energy stored in fiber and matrix are calculated separately in terms of overall deformation of the unit cell (δ, L_y, L_x).

$$U_{tot} = U_{Mt} + U_{Mb} + U_{ft} + U_{fb} + U_{st} + U_{sb} \tag{30}$$

Since $U_{st} = 2A_s S_{x0}(A_{1-D})$ in the unit cell, then:

$$\begin{aligned} U_{tot} &= U_{Mt} + U_{Mb} + U_{ft}^y + U_{fb}^y + 2A_s S_{x0} \times A_{1-D} + U_{sb}^x \\ &= \frac{E_m V_0}{2(1 - \mu_m^2)} (E_{11}^2 + E_{22}^2 + 2\mu_m E_{11} E_{22}) \\ &+ 2D\pi^4 \left(\frac{1}{L_{x0}^2} + \frac{1}{L_{y0}^2}\right)^2 L_{x0} L_{y0} \delta^2 \\ &+ 2A_f S_{y0} \left(\frac{1}{2} E_f \varepsilon_{fy}^2 + \frac{1}{4} E_{f3} \varepsilon_{fy}^4 + \frac{1}{6} E_{f5} \varepsilon_{fy}^6\right) \\ &+ 768 \frac{E_f I_f}{S_{y0}^3} \delta^2 + 2A_s S_{x0} (A_{1-D}) + 768 \frac{E_s I_s}{S_{x0}^3} \delta^2 \end{aligned} \tag{31}$$

where U_{Mt} , U_{Mb} , U_{ft}^y , U_{fb}^y , and U_{sb}^x , are tension strain energy in matrix, bending strain energy in matrix,

tension strain energy in elastic yarns, bending strain energy in elastic yarns and bending strain energy in SMA fibers neglecting thermal and phase deformation effects. A_s is the cross sectional area of a SMA wire and A_{1-D} is total Helmholtz free energy for a SMA wire per unit volume (Eq. 26).

5 Constitutive equations for a smart unit cell

Using Principle of Total Potential Energy (Ugural 1990), we have:

$$\Pi_{11} = \frac{1}{V} \frac{\partial U_{tot}}{\partial g_{11}}, \quad \Pi_{22} = \frac{1}{V} \frac{\partial U_{tot}}{\partial g_{22}}, \quad \text{and} \quad 0 = \frac{\partial U_{tot}}{\partial \delta} \tag{32}$$

where Π_{ij} are the Lagrangian Stress components and $V = L_{x0}L_{y0}t_0$.

Therefore:

$$\Pi_{11} = \frac{1}{V} \left(\frac{\partial U_{tot}}{\partial \varepsilon_{fx}} \frac{\partial \varepsilon_{fx}}{\partial g_{11}} + \frac{\partial U_{tot}}{\partial \varepsilon_{fy}} \frac{\partial \varepsilon_{fy}}{\partial g_{11}} \right) \tag{33a}$$

$$\Pi_{22} = \frac{1}{V} \left(\frac{\partial U_{tot}}{\partial \varepsilon_{fx}} \frac{\partial \varepsilon_{fx}}{\partial g_{22}} + \frac{\partial U_{tot}}{\partial \varepsilon_{fy}} \frac{\partial \varepsilon_{fy}}{\partial g_{22}} \right) \tag{33b}$$

$$0 = \frac{\partial U_{tot}}{\partial \delta} \tag{33c}$$

then

$$\Pi_{11} = \frac{1}{V} \left\{ \frac{\partial U_{Mt}}{\partial E_{11}} \frac{\partial E_{11}}{\partial g_{11}} + \frac{\partial U_{Mt}}{\partial E_{22}} \frac{\partial E_{22}}{\partial g_{11}} + \frac{\partial U_{ft}}{\partial \varepsilon_{fx}} \frac{\partial \varepsilon_{fx}}{\partial g_{11}} + \frac{\partial U_{ft}}{\partial \varepsilon_{fy}} \frac{\partial \varepsilon_{fy}}{\partial g_{11}} + 2A_s S_{x0} \left(\frac{\partial A_{1-D}}{\partial \varepsilon_{fx}} \frac{\partial \varepsilon_{fx}}{\partial g_{11}} + \frac{\partial A_{1-D}}{\partial \varepsilon_{fy}} \frac{\partial \varepsilon_{fy}}{\partial g_{11}} \right) \right\} \tag{34a}$$

$$\Pi_{22} = \frac{1}{V} \left\{ \frac{\partial U_{Mt}}{\partial E_{11}} \frac{\partial E_{11}}{\partial g_{22}} + \frac{\partial U_{Mt}}{\partial E_{22}} \frac{\partial E_{22}}{\partial g_{22}} + \frac{\partial U_{ft}}{\partial \varepsilon_{fx}} \frac{\partial \varepsilon_{fx}}{\partial g_{22}} + \frac{\partial U_{ft}}{\partial \varepsilon_{fy}} \frac{\partial \varepsilon_{fy}}{\partial g_{22}} + 2A_s S_{x0} \left(\frac{\partial A_{1-D}}{\partial \varepsilon_{fx}} \frac{\partial \varepsilon_{fx}}{\partial g_{22}} + \frac{\partial A_{1-D}}{\partial \varepsilon_{fy}} \frac{\partial \varepsilon_{fy}}{\partial g_{22}} \right) \right\} \tag{34b}$$

$$0 = \left\{ \frac{\partial U_{Mb}}{\partial \delta} + \frac{\partial U_{ft}}{\partial \varepsilon_{fx}} \frac{\partial \varepsilon_{fx}}{\partial \delta} + \frac{\partial U_{ft}}{\partial \varepsilon_{fy}} \frac{\partial \varepsilon_{fy}}{\partial \delta} + \frac{\partial U_{fb}}{\partial \delta} + \frac{\partial U_{sb}}{\partial \delta} + 2A_s S_{x0} \left(\frac{\partial A_{1-D}}{\partial \varepsilon_{fx}} \frac{\partial \varepsilon_{fx}}{\partial \delta} + \frac{\partial A_{1-D}}{\partial \varepsilon_{fy}} \frac{\partial \varepsilon_{fy}}{\partial \delta} \right) \right\} \tag{34c}$$

then

$$\Pi_{11} = \frac{1}{V} \left\{ 2A_s \left(\frac{\partial A_{1-D}}{\partial \varepsilon_{fx}} \right) \left(\frac{\partial S_x}{\partial g_{11}} \right) + \left(\frac{\partial U_{Mt}}{\partial E_{11}} \right) \cdot g_{11} \right\} \tag{35a}$$

$$\Pi_{22} = \frac{1}{V} \left\{ \frac{1}{S_{y0}} \left(\frac{\partial U_{ft}}{\partial \varepsilon_{fy}} \right) \left(\frac{\partial S_y}{\partial g_{22}} \right) + \left(\frac{\partial U_{Mt}}{\partial E_{22}} \right) \cdot g_{22} \right\} \tag{35b}$$

$$0 = \left\{ 2A_s \frac{\partial A_{1-D}}{\partial \varepsilon_{fx}} \frac{\partial S_x}{\partial \delta} + \frac{1}{S_{y0}} \frac{\partial U_{ft}}{\partial \varepsilon_{fy}} \frac{\partial S_y}{\partial \delta} \right. \\ \left. \frac{\partial U_{fb}}{\partial \delta} + \frac{\partial U_{sb}}{\partial \delta} + \frac{\partial U_{Mb}}{\partial \delta} \right\} \tag{35c}$$

and the final constitutive equations for SSMAWC obtained as:

$$\Pi_{11} = \frac{1}{V} \left\{ \alpha_s \cdot \frac{\partial S_x}{\partial g_{11}} + W_{11} g_{11} \right\} \tag{36a}$$

$$\Pi_{22} = \frac{1}{V} \left\{ \beta_y \frac{\partial S_y}{\partial g_{22}} + W_{22} g_{22} \right\} \tag{36b}$$

$$0 = \alpha_s \frac{\partial S_x}{\partial \delta} + \beta_y \frac{\partial S_y}{\partial \delta} + 1536 \left(\frac{E_f I_f}{S_{y0}^3} + \frac{E_s I_s}{S_{x0}^3} \right) \delta \\ + 4D\pi^4 \left(\frac{1}{L_{x0}^2} + \frac{1}{L_{y0}^2} \right)^2 L_{x0} L_{y0} \delta \tag{36c}$$

in which:

$$\alpha_s = 2A_s \left(\frac{\partial A_{1-D}}{\partial \varepsilon_{fx}} \right) = 2A_s \left(\frac{\partial A_{1-D}}{\partial \varepsilon_x} \right) \tag{37}$$

From Eq. 26:

$$\alpha_s = 2A_s(\sigma_x) = 2A_s \left(\frac{\partial A_{1-D}}{\partial \varepsilon_x} \right) = 2A_s \left\{ \left(\frac{\partial^2 A_{1-D}}{\partial \varepsilon_x^2} \right) \Big|_{Q_0} \right. \\ \times (\varepsilon_x - \varepsilon_{x0}) + \left(\frac{\partial^2 A_{1-D}}{\partial \varepsilon_x \partial \zeta} \right) \Big|_{Q_0} \\ \times (\zeta - \zeta_0) + \left(\frac{\partial^2 A_{1-D}}{\partial T \partial \varepsilon_x} \right) \Big|_{Q_0} (T - T_0) \left. \right\} \tag{38}$$

we know from Brinson’s formulation (Brinson 1999) that:

$$\left(\frac{\partial^2 A_{1-D}}{\partial \varepsilon_x^2}\right)\Bigg|_{Q_0} = E(\varepsilon, T, \zeta) = E(\zeta) = E_A + \zeta(E_M - E_A) \tag{39}$$

$$\left(\frac{\partial^2 A_{1-D}}{\partial T \partial \varepsilon_x}\right)\Bigg|_{Q_0} = \theta(\varepsilon, T, \zeta) = \theta \tag{40}$$

$$\left(\frac{\partial^2 A_{1-D}}{\partial \varepsilon_x \partial \zeta}\right)\Bigg|_{Q_0} = \psi(\varepsilon, T, \zeta) = -\varepsilon_L E(\zeta) \tag{41}$$

So we have:

$$\alpha_S = 2A_S \{ E(\zeta) \times (\varepsilon_x - \varepsilon_{x0}) - \varepsilon_L \times E(\zeta) \times (\zeta - \zeta_0) + \theta(T - T_0) \} \tag{42}$$

and:

$$\beta_y = \frac{1}{S_{y0}} \left(\frac{\partial U_{ft}}{\partial \varepsilon_{fy}}\right) = 2A_f (E_f \varepsilon_{fy} + E_{f3} \varepsilon_{fy}^3 + E_{f5} \varepsilon_{fy}^5) \tag{43}$$

$$\frac{\partial S_x}{\partial g_{11}} = L_{x0} \left(1 - 9.6 \left(\frac{a_x}{L_x}\right)^2 + 147.6 \left(\frac{a_x}{L_x}\right)^4 \right) \tag{44}$$

$$\frac{\partial S_y}{\partial g_{22}} = L_{y0} \left(1 - 9.6 \left(\frac{a_y}{L_y}\right)^2 + 147.6 \left(\frac{a_y}{L_y}\right)^4 \right) \tag{45}$$

$$\frac{\partial S_x}{\partial \delta} = 19.2 \left(\frac{a_x}{L_x}\right) - 196.8 \left(\frac{a_x}{L_x}\right)^3 \tag{46}$$

$$\frac{\partial S_y}{\partial \delta} = 19.2 \left(\frac{a_y}{L_y}\right) - 196.8 \left(\frac{a_y}{L_y}\right)^3 \tag{47}$$

$$W_{11} = \frac{E_m V_0}{(1 - \mu_m^2)} (E_{11} - \mu_m E_{22}) \tag{48}$$

$$W_{22} = \frac{E_m V_0}{(1 - \mu_m^2)} (E_{22} - \mu_m E_{11}) \tag{49}$$

6 Case studies, results and discussions

The developed nonlinear equation does not have closed form solution. It contains three nonlinear equations and seven variables: L_x , L_y , δ , Π_{11} , Π_{22} , T , and ζ . Two variables T and ζ are defined using constitutive relations for SMAs depicted by Brinson (1999) and Brinson and Lammering (1993). Thus, once any other two of these variables are specified, the remaining three unknowns can be solved numerically.

A computer program has been developed using Matlab workspace to solve these equations. The program uses the material and geometrical properties of the constituents within the composite as well as temperature as input arguments. During the run time, the Lagrangian stresses components are accepted as inputs. A modified version of this program accepts deformation gradients (or strain components) to solve for the Lagrangian stress components. The material parameters of the matrix, Nylon fibers and SMA in the numerical example are listed in Tables 1 and 2. The material properties of the constituents are listed in Tables 3 and 4. In order to solve the above relations, in this section, a smart shape memory alloy woven unit cell (Fig. 1) is considered under two types of applied uniform loadings, namely: uniform biaxial loading (case I) and uniform uniaxial loading (case II).

The results for the unit cell starts at initial temperature of 5°C. By increasing temperature in each case, deformation of composite according to applied uniform load and temperature was plotted, that are shown in following figures. Increasing the temperature results a Martensite–Austenite transformation from the temperature below the A_s (Austenite start) up to A_f (Austenite final). Martensite Fraction Coefficient (ζ) varies during temperature raising (Martensite to Austenite transformation) that is shown for all cases in Fig. 2 by continuous line. The dashed line illustrates the Martensite Fraction Coefficient (ζ) when temperature is decreased (Austenite to Martensite transformation).

As it can be inferred from Fig. 2, Martensite–Austenite transformation has been completed above the A_f temperature and 18% tension and 18% compression can be seen in both x and y directions. The dashed lines illustrate the unit cell behavior when temperature is decreased (Austenite to Martensite transformation). A 3D illustration for the deformation of the unit cell under temperature and uniform

Table 1 Material properties for matrix (SILGARD-184)

E_m (MPa)	1.69
ρ (kg/m ³)	1050
σ_y/τ_y (MPa)	108/0.104
Elongation (%)	100
Useful temperature range (°C)	–55–200
ν_m	0.46

Table 2 Mechanical properties for shape memory alloy (Nitinol) (Brocca et al. (1999))

Module density	Transformation temperatures (°C)	Transformation constants	Other
$D_a = 67 \times 10^3$ MPa	$M_f = 9$	$C_M = 8$ MPa/°C	Max. residual strain $\epsilon_L = 0.067$
$D_m = 26.3 \times 10^3$ MPa	$M_s = 18.4$	$C_A = 13.8$ MPa/°C	Resistivity $\rho_e = 0.9 \times 10^{-6}$
$\Phi = 0.55$ MPa/°C	$A_s = 34.5$	$\sigma_s^{cr} = 100$ MPa	Specific heat $C_p = 920$ J/kg°C
$\rho = 6500$ kg/m ³	$A_f = 49$	$\sigma_f^{cr} = 170$ MPa	Conductivity $\chi = 18$ W/m°C

Table 3 Material properties for elastic fibers (Nylon 728)

Ex_1 (MPa)	1200
Ey_1 (MPa)	2270
Ex_1 (MPa)	-151,000
ν_f	0.40

Table 4 Geometrical properties for unit cell

a_{x0} (mm)	0.287
a_{y0} (mm)	0.258
L_{x0} (mm)	2.254
L_{y0} (mm)	2.342
t (mm)	1.65
r_x (mm)	0.254
r_y (mm)	0.255
S_{x0} (mm)	2.275
S_{y0} (mm)	2.558
V_0 (m ³)	$t \times L_{x0} \times L_{y0}$

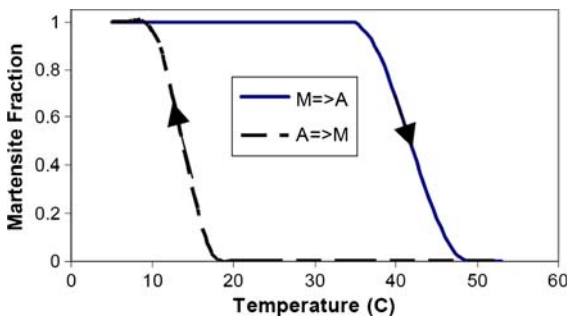


Fig. 2 Martensite fraction versus temperature

uniaxial loading variation (Martensite to Austenite transformation), is demonstrated in Figs. 3 and 4.

For the second loading condition (case II) the result is shown in the Fig. 5. in this case uniform uniaxial stress is applied in x direction. The Martensite Fraction Coefficient versus temperature is shown in Fig. 2. Although the phase transformation temperature varies vs. applied stress, but the stress variation is less than that the phase transformation temperature

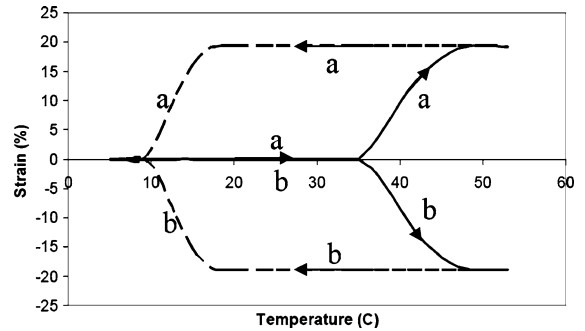


Fig. 3 Temperature dependent strains diagram for both x and y directions obtained by raising temperature under uniform biaxial loading

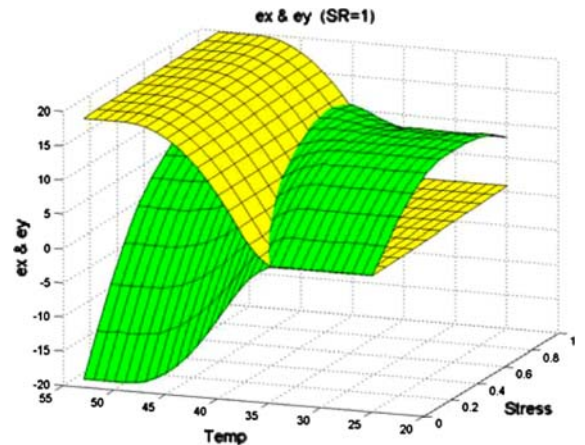


Fig. 4 3D illustration for the deformation of the unit cell under temperature and uniform biaxial loading variation (Martensite to Austenite transformation), yellow diagram for x direction and green one for y direction, Stress (MPa), Temp (C), Strain (%)

could affect the results (Brinson 1999 and Brinson and Lammering 1993). Therefore, it is assumed that Fig. 2 is valid for all stress ranges. From Fig. 2, it can be inferred that this variation is less than one centigrade degree per 1 MPa. Since no external loading is applied in y direction, therefore, only the

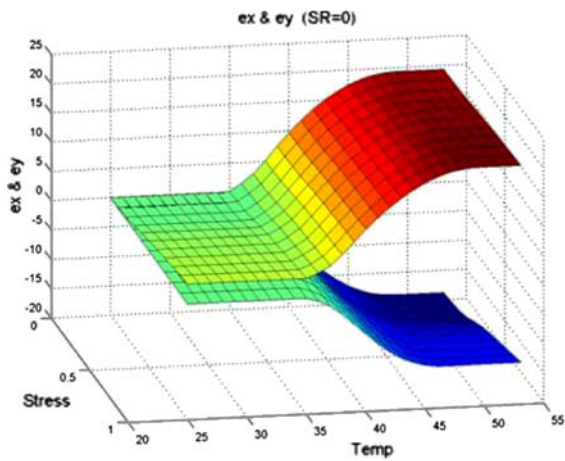


Fig. 5 3D illustration for the deformation of the unit cell under temperature and uniform uniaxial loading variation (Martensite to Austenite transformation), positive data for *x* direction and negative data for *y* direction Stress (MPa), Temp (C), Strain (%)

displacement of contact point causes the deformation in the *y* direction.

To validate the numerical results of Eq. 36, a 3D finite element model for unit cell was developed in ANSYS workspace. Using element Link185 and generating an ANSYS program, results under uniaxial loading was obtained. The results in the case in which $\prod_{22} = 0$ (uniaxial loading) are illustrated in Table 5 (temperature is considered to be constant = 7°C < Af & Ms). As one can see from Table 5, the obtained results from the proposed analytical method correspond closely with the results of the presented FEM solution. Furthermore, the maximum difference between the analytical solution

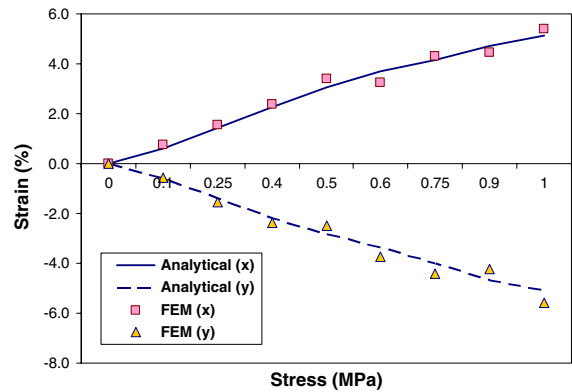


Fig. 6 Strain–Stress diagram, comparison between analytical and FEM results (temperature is considered to be constant = 7°C)

and FEM is about 15.7% for fill (*x*) direction and 11.9% for warp (*y*) direction. In order to illustrate these results, Fig. 6 also shows the stress–strain curves of the composite under the above mentioned conditions.

7 Conclusions

A theoretical micro-mechanical model is developed in the present paper for SSMAWCs under combined biaxial tensile deformation. The framework of the approach consists of the geometric model of a unit cell, and the strain energy based constitutive equations under large deformation.

The modeling strategy starts with a geometrical description of the yarn and the unit cell. The shape and the area of the cross section of fibers are assumed

Table 5 Deformation of composite under uniaxial loading in both fill and warp direction

Stress (MPa)	Present FEM		Present analytical		Difference (%)	
	Strain (%) fill (0°)	Strain (%) warp (90°)	Strain (%) fill (0°)	Strain (%) warp (90°)	Fill direction	Warp direction
0.00	0.0000	0.0000	0.0000	0.0000	0.0	0.0
0.10	0.6158	−0.6103	0.7210	−0.5500	15.7	10.4
0.25	1.4228	−1.3940	1.5600	−1.5380	9.2	9.8
0.40	2.2744	−2.1960	2.3900	−2.3920	5.0	8.5
0.50	3.0640	−2.8168	3.3900	−2.5000	10.1	11.9
0.60	3.6859	−3.3610	3.2500	−3.7220	12.6	10.2
0.75	4.1596	−4.0060	4.3200	−4.4300	3.8	10.1
0.90	4.7197	−4.6690	4.4400	−4.2350	6.1	9.7
1.00	5.1158	−5.1103	5.3910	−5.5700	5.2	8.6

to be the same along the yarn direction in sinusoidal shape. Yarns are pinned together at the crossover points and the matrix and metal layers are completely stuck. In addition, no friction is assumed between yarns. Under these assumptions, the micromechanical analysis of the unit cell is provided. One-dimensional Helmholtz free energy relation for SMA fibers are developed. In this way, based on the first and second law of thermodynamics and Maxwell relations, variations of main parameters about some equilibrium (initial) values, were examined by using a Taylor series approximation.

By such an analysis it is intended to form an opinion about thermo-elastic behavior of laminated plates used in engineering problems associated with such structural designs. Using kinetic relations of SMA fibers, depicted by Brinson (1999) and Brinson and Lammering (1993), some numerical studies are carried out in order to solve the final constitutive equations, in some arbitrary cases.

References

- Boisse, P., Borr, M., Cherouat, A.: Finite element simulation of textile composite forming including the biaxial fabric behavior. *Compos Part B: Eng.* **28B**(4), 453–464 (1997)
- Brinson, L.C., Lammering, R.: Finite element analysis of the behavior of shape memory alloys and their applications. *Int. J. Solids Struct.* **30**(23), 3261–3280 (1993)
- Brinson, L.C., Bekker, A., Hwang, S.: Deformation of shape memory alloy due to thermo-induced transformation. *J. Intell. Mater. Syst. Struct.* **7**, 97–107 (1996)
- Brocca, M., Brinson, L.C., Bazant, Z.P.: Three dimensional constitutive model for shape memory alloys based on microplane model. *J. Mech. Phys. Solids.* **50**, 1051–1077 (1999)
- Chamis, C.C., Sendekyj, G.P.: Critique on theories predicting thermoelastic properties of fibrous composites. *J. Compos. Mater* **2**, 332–358 (1968)
- Dano, M.-L., Hyer, M.W.: SMA-induced snap-through of unsymmetric fiber-reinforced composite laminates. *Int. J. Solids Struct.* **40**, 5949–5972 (2003)
- Gao, X., Huang, M., Brinson, L.C.: A multivariant micromechanical model for SMAs Part 1 Crystallographic issues for single crystal model. *Int. J. Plast.* **16**, 1345–1369 (2000a). doi:[10.1016/S0749-6419\(00\)00013-9](https://doi.org/10.1016/S0749-6419(00)00013-9)
- Gao, X., Huang, M., Brinson, L.C.: A multivariant micromechanical model for SMAs part 2 polycrystal model. *Int. J. Plast.* **16**, 1345–1369 (2000b). doi:[10.1016/S0749-6419\(00\)00013-9](https://doi.org/10.1016/S0749-6419(00)00013-9)
- Gao, X., Catherine, B. L.: A simplified multivariant SMA model based on invariant plane nature of martensitic transformation, Northwestern University, Technical notes (2002)
- Halpin, J.C.: Primer on Composite Materials Analysis, 2nd edn., pp. 153–192. Technomic, Lancaster (1992)
- Hashin, Z.: Analysis of properties of fiber composites with anisotropic constituents. *J. Appl. Mech.* **46**, 453–550 (1979)
- Hashin, Z.: Analysis of composite materials—a survey. *J. Appl. Mech.* **50**, 481 (1983)
- Hsiao, S.W., Kikuchi, N.: Numerical analysis and optimal design of composite thermoforming process. *Comput. Meth Appl Mech Eng.* **177**, 1–34 (1999)
- Kawai, M., Ogawa, H., Baburaj, V., Koga, T.: Micromechanical analysis for hysteretic behavior of unidirectional TiNi SMA fiber composites. *J. Intell. Mater. Struct.* **10**, 14 (1999)
- Khalili, S.M.R., Shokuhfar, A., Malekzadeh, K., Ashenai Ghasemi, F.: Low-velocity impact response of active thin-walled hybrid composite structures embedded with SMA wires. *Thin-Walled Struct.* **45**, 799–808 (2007a)
- Khalili, S.M.R., Shokuhfar, A., Ashenai Ghasemi, F.: Effect of smart stiffening procedure on low-velocity impact response of smart structures. *J. Mater. Process. Technol.* **190**, 142–152 (2007b)
- Kollegal, M.G., Sridharan, S.: Strength prediction of plain woven fabrics. *J. Compos. Mater.* **34**(3), 240–257 (2000)
- Lagoudas, D.C., Boyd, J.G., Bo, Z.: Micromechanics of active composites with SMA fibers. *Trans. ASME Eng. Mat. Tech* **116**, 337 (1994)
- Luo, S., Chou, S.W.: Modeling of nonlinear elastic behavior of elastomeric flexible composites, The 192nd National Meeting of the American Chemical Society. Anaheim, California (1986)
- Luo, S., Mitra, A.: An experimental study of biaxial behavior of flexible fabric composite. In: Gibson, R.F., Chuo, T.W., Rajo, P.K. (eds.) *Innovative proceeding and characterization of composite material*, pp. 317–328. ASME, New York (1995a)
- Luo, S., Mitra, A.: Finite elastic behavior of flexible fabric composite under biaxial loading. *J. Appl. Mech.* **66**, 631–638 (1995b)
- McCullough, R.L.: Micro-models for composite materials—continuous fiber composites, micromechanical materials modeling. In: Whitney, J.M., McCullough, R.L. (eds.) *Delaware composites design encyclopedia*, vol. 2. Technomic, Lancaster (1990)
- Murasawa, G., Tohgo, K., Ishii, H.: Deformation behavior of NiTi/polymer shape memory alloy composites—experimental verifications. *J. Compos. Mater* **38**, 399 (2004)
- Peng, X.Q., Cao, J.: A dual homogenization and finite element approach for material characterization of textile composites. *Compos. Part B* **33**(1), 45–56 (2002)
- Ugural, A.C.: *Stresses in plates and shells*. Wiley, New York (1990)
- Xue, P., Peng, X.Q., Cao, J.: A non-orthogonal constitutive model for characterizing woven composite. *Compos Part A Appl. Sci. Manuf.* **34**(2), 183–193 (2003)
- Xue, P., Cao, J., Chen, J.: Integrated micro macro/mechanical model of woven fabric composites under large deformation. *Compos. Struct.* **70**, 69–80 (2005)

Yongsheng, R., Shuangshuang, S.: Large amplitude flexural vibration of the orthotropic composite plate embedded with shape memory alloy fibers. *Chin. J. Aeronautics* **20**, 415–424 (2007)

Zhou, G., Sim, L.M., Brewster, P.A., Giles, A.R.: Through-the-thickness mechanical properties of smart quasi-isotropic carbon/epoxy laminates. *Compos. Part A* **35**, 797–815 (2004)